Supporting Information for

"Time-Resolved Small-Angle X-Ray Scattering Reveals Millisecond Transitions of a DNA Origami Switch"

Linda K. Bruetzel[1,†], Philipp U. Walker[1,†], Thomas Gerling[2], Hendrik Dietz[2], Jan Lipfert[1,*]

[1]Department of Physics, Nanosystems Initiative Munich, and Center for Nanoscience, LMU Munich, Amalienstrasse 54, 80799 Munich, Germany

[2]Physik Department, Walter Schottky Institute, Technische Universität München, Am Coulombwall 4a, 85748 Garching near Munich, Germany

[†]These authors contributed equally to this work.

[*]Corresponding author: E-mail: Jan.Lipfert@lmu.de. Phone: +49-89-2180-2005

Supporting Information consisting of

- **Materials and Methods**
- **Supporting Text**
- **Supporting Figures S1-S8**
- **Supporting References**

MATERIALS AND METHODS

DNA origami assembly and purification. The scaffold DNA (p8064) was prepared as previously described.[1] Staple DNA strands were synthesized by solid-phase chemical synthesis (Eurofins Genomics GmbH, Ebersberg, Germany; HPSF purification). DNA origami objects were designed using caDNAno v.02[2] and prepared as described previously.[3, 4] Objects were self-assembled by subjecting the one-pot reaction mixture to a thermal annealing ramp using a thermal cycling device (TETRAD; MJ Research – now Biorad).[5] The reaction mixture contained 50 nM scaffold DNA (p8064), 200 nM of each staple DNA strand, folding buffer (1 mM EDTA, 5 mM TrisBase, 5 mM NaCl; pH 8), and 20 mM $MgCl_2$.

DNA origami switch device. All 16 basepair stacking interactions are active in the dynamic switch variant switchD16 (**Supporting Figure S6**). After a 15 min thermal denaturation step at 65 ˚C, the thermal annealing ramp covered the temperature interval [58 – 55 ˚C] with a rate of 1 ˚C/90 min.

Excess staple DNA strands were removed from the reaction mixture by performing two rounds of polyethylene glycol (PEG) precipitation.[6] The resulting pellet was dissolved in folding buffer (1 mM EDTA, 5 mM TrisBase, 5 mM NaCl; pH 8) containing 5 mM $MgCl_2$. To allow for equilibration, all samples were incubated at 40 ˚C and 400 rpm overnight. Residual PEG was removed from the samples by performing three rounds of ultrafiltration (30K Amicon Ultra-0.5mL from Merck Millipore). Filters were equilibrated by adding 500 µL folding buffer containing 5 mM $MgCl_2$ at 2000 x g and 25 ˚C for 2 minutes. Then, 50 µL sample was mixed with 450 µL folding buffer and centrifuged at 8000 x g and 25 ˚C for 15 minutes. The flow-throw was discarded and 480 µl of folding buffer was added to the recovered sample.

DNA origami bricks. We used a self-complementary DNA origami brick where the protrusions on its front face can click into correspondingly shaped recessions on its back face. Two samples were prepared: in brick A1 protrusions are active and recessions were permanently deactivated (**Supporting Figure S7**) and in brick A2 recessions are active and protrusions were permanently deactivated (**Supporting Figure S8**). Blunt end contacts were permanently deactivated by using 10-thymine-long overhangs. After a 15 min thermal denaturation step at 65 ˚C, the thermal annealing ramp covered the temperature interval [56 – 50 ˚C] with a rate of 1 ˚C/60 min.

Excess staple DNA strands were removed from the reaction mixture by performing one round of polyethylene glycol (PEG) precipitation.[6] The resulting pellets were dissolved in HPLC buffer (1 mM EDTA, 5 mM TrisBase, 200 mM NaCl; pH 8) containing 5 mM $MgCl_2$. Then, we subjected the sample to HPLC (Agilent Technologies 1260/1290 Infinity) using the column (Agilent Bio SEC-5: 5 μm; 2000A; 21.2 x 300 mm) at a flow rate of 2 ml/min and collected fractions of the monomer peak (29.5 – 33.5 minutes). Due to dilution of the sample, we used ultrafiltration (30K Amicon Ultra-15mL from Merck Millipore) to concentrate the sample and to exchange the buffer to folding buffer (1 mM EDTA, 5 mM TrisBase, 5 mM NaCl; 5 mM $MgCl_2$; pH 8). Filters were equilibrated by adding 15 ml folding buffer containing 5 mM $MgCl_2$ at 7000 x g and 25 ˚C for 5 minutes. Then, 15 ml sample was added and centrifuged at 7000 x g and 25 ˚C for 7 minutes. The flow through was discarded. This step was repeated until the entire volume of the sample was centrifuged in the same filter. Then, the sample was mixed with 15 ml folding buffer and centrifuged at 7000 x g and 25 ˚C for 7 minutes. This step was repeated three times. The concentration of all DNA origami samples was determined using a spectrophotometer (NanoDrop 8000; Thermo Scientific). All SAXS experiments were performed on SwitchD16 and brick samples dissolved in folding buffer (1 mM EDTA, 5 mM TrisBase, 5 mM NaCl; pH 8) containing varying $MgCl_2$ concentrations.

SAXS data acquisition

SAXS measurements were performed at beamline P12, DESY, Hamburg[7] and the high brilliance SAXS beamline ID02, ESRF[8], Grenoble.

P12. SAXS measurements at beamline P12 were performed at an X-ray wavelength λ of 1.2 Å and a sample-to-detector distance of 3.0 m, resulting in a q-range of 0.03 to 5 nm^{-1} (with $q = 4\pi·\sin(\theta)/\lambda$, where 2θ is the total scattering angle). For data acquisition we used a Pilatus 2M detector. For each sample condition 40 frames with an exposure time of 45 ms in 'flow' mode were conducted at room temperature. Buffer samples were measured using identical procedures before and after each sample measurement. Static profiles of monomeric and heterodimeric brick constructs were measured in buffer with 20 mM $MgCl_2$ at sample concentrations of 50 nM and 100 nM, respectively. Time-resolved (tr) SAXS measurements on dimerization kinetics were performed by manual mixing of 50 nM and 100 nM monomer concentrations in a 1:1 mixing ratio.

ID02. SAXS experiments were performed at an X-ray wavelength λ of 0.99 Å. Static experiments at beamline ID02 on switchD16 samples and DNA origami brick monomer and dimer samples were performed in a temperature controlled flow through capillary operated in air using the Rayonix MX-170HS detector (Rayonix L.L.C., USA) with a sample-to-detector distance of 5 m resulting in a *q*-range of 0.015 nm^{-1} to 1.5 nm^{-1}. Data acquisition was performed with an exposure time of 10 ms including 50 repeats and a delay time of 0.5 s in order to reduce radiation damage. The measurements were conducted at room temperature. SwitchD16 samples were measured at a final sample concentration of 100 nM.

TrSAXS experiments on switchD16 samples were conducted using a stopped-flow device (SFM-400, Bio-Logic, Claix, France) consisting of four motorized syringes coupled through three mixers. The last mixer is coupled to a quartz capillary with a diameter of 1.5 mm that serves as the observation volume where the sample is exposed to the X-ray beam at a constant position (**Figure 1a**). A hard-stop is placed at the end of the flow line and is activated at the end of the mixing sequence in order to stop the flow. The net dead time (~ 1 ms) including the mixing time and the time to transfer the mixture to the beam crossing point in the capillary was determined as described elsewhere[8]. For each trSAXS measurement 150 µl each of buffer and switchD16 samples were prepared in the syringes for mixing and subsequently mixed at equal volumes. For stopped-flow based SAXS experiments the sample-to detector distance was set to 2.5 m covering a *q*-range of 0.04 nm^{-1} to 3.0 nm^{-1}. For each run 30 to 50 frames were recorded with an exposure time of 10 ms and a delay time $t_d = (16 \times 1.05^i)$ ms (where *i* denotes the actual frame number) between consecutive frames in order to prevent radiation damage. For trSAXS experiments switchD16 samples at a concentration of 200 nM were dissolved in 5 mM MgCl$_2$ buffer. Buffer solutions with MgCl$_2$ concentrations of 65 mM, 45 mM, 25mM, and 5 mM were prepared to achieve final MgCl$_2$ concentrations after mixing of 35 mM, 25 mM, 15 mM and 5 mM, respectively. Prior to each stopped-flow experiment static profiles of switchD16 samples (c = 100 nM) at 5 mM, 15 mM, 25 mM and 35 mM MgCl$_2$ concentrations and corresponding buffer profiles were recorded with the exposure time set to 10 ms and the number of frames to 10. For each MgCl$_2$ concentration two independent trSAXS repeats were conducted.

SAXS data processing

Data reduction was carried out using custom written scripts in Matlab (Matlab 2015, The MathWorks Inc., Natick, MA, USA). Scattering data were normalized to the intensity at zero angles (*I(0)*) by performing Guinier analysis of the data.[9]

Static SAXS measurements. For static SAXS experiments performed at beamline P12 and ID02, sample and buffer data from each run were analyzed for radiation damage, which was not observed in any of the measurement. Matching sample and buffer profiles were averaged and buffer profiles were subtracted for background correction.

Stopped-flow based SAXS measurements. For each $MgCl_2$ concentration scattering profiles at each acquisition point were checked for consistency and radiation damage; no damage was observed in any of the measurements. Matching averaged buffer profiles from static SAXS experiments were subtracted from each single frame for background correction.

SAXS data analysis

SwitchD16. For trSAXS data, the scattering profile at each acquisition point (*I(q,t)*) can be described by a superposition of the scattering profiles of the sample conformation at the initial solution condition (*$I_i(q,t_o)$*) before mixing and the scattering profile of the final state at equilibrium after mixing (*$I_f(q,t_{eq})$*):

$$I(q,t) = f_i \cdot I_i(q,t_o) + f_f \cdot I_f(q,t_{eq}) \tag{1}$$

where the coefficients f_i and f_f are fractional occupancies of the initial and final states. For stopped-flow experiments we used static reference profiles of switchD16 samples acquired at 5 mM $MgCl_2$ and 15 mM, 25 mM and 35 mM $MgCl_2$ concentrations for I_i and I_f, respectively. For some frames, portions of the scattering curves deemed unreliable at the lowest *q*-values due to parasitic scattering and at high *q*-values because of low signal-to-noise ratio resulting in an utilizable *q*-range of 0.08 nm^{-1} to 2.5 nm^{-1} for fitting. The fraction of closed particles was determined from two independent SAXS measurements at each $MgCl_2$ concentration and time point and the mean and the standard deviation were calculated and reported in Figure 2b. Fraction of closed particles were normalized to the portion of closed switchD16 particles in steady state for each $MgCl_2$ concentration (i.e. 0 %, 90%, 98% and 99 % for 5 mM, 15 mM, 25 mM and 35 mM $MgCl_2$ concentrations, respectively), derived from previous SAXS

measurements.[4] To evaluate the goodness of the two-state fits, *chi*-squared values (χ^2) were calculated for each fit according to the following equation:

$$\chi^2 = \sum_i \frac{[I_{exp}(q_i,t) - I_{fit}(q_i,t)]^2}{\sigma_i^2} \tag{2}$$

where I_{exp} is the experimental SAXS profile, I_{fit} the best two-state fit profile, and σ the experimental error of I_{exp}.

Bricks. Two-state fits for dimerization kinetics of DNA origami bricks were performed using Equation 1, where the initial and final state are given by the scattering profiles of the monomer at the respective starting concentration and the dimer at equilibrium. Each fit was evaluated according to Equation 2. To determine the fraction of dimers, we used the *q*-range from 0.1 to 2.5 nm^{-1}.

Kinetic fits for folding and assembly.

SwitchD16. The (intramolecular) conformational change between the open and the closed state of the switchD16 sample was modelled as a reversible first-order reaction:

$$O \underset{k_{open}}{\overset{k_{close}}{\rightleftharpoons}} C \tag{3}$$

where O and C denote the open and closed state of switchD16 particles and k_{close} and k_{open} describe the closing and opening rate constants. Assuming that all objects (with an initial concentration of c_0) adopt an open conformation at $t_0 = 0$, the time dependent relative concentrations of particles in the open and closed state are given by:

$$\frac{c_O(t)}{c_0} = \frac{k_{open} + k_{close}e^{-(k_{close}+k_{open})t}}{k_{close} + k_{open}} \tag{4}$$

$$\frac{c_C(t)}{c_0} = \frac{k_{close} - k_{close}e^{-(k_{close}+k_{open})t}}{k_{close} + k_{open}} \tag{5}$$

The equilibrium constant K_{eq} of the reaction is defined as:

$$K_{eq} = \frac{k_{close}}{k_{open}} = \exp\left(-\frac{\Delta G}{k_B T}\right) \tag{6}$$

where k_B is the Boltzmann constant and ΔG denotes the Gibb´s free energy between the open and the closed state.
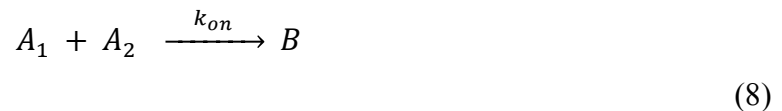
To estimate the closing rate constants for the 25 mM and 35 mM MgCl$_2$ data, we calculated the fraction of closed particles following Equation 5 for different closing rate constants (20 s^{-1} < k_{close} < 300 s^{-1}) with k_{open} = 0 (as at MgCl$_2$ concentrations of 25 mM and

35 mM the closed fractions in equilibrium are ~98 % and ~99 %, respectively, suggesting that the opening rate constant is essentially negligible) and calculated the reduced χ^2-values for each closing rate constant given by:

$$\chi^2_{red} = \frac{1}{N}\left(\sum_i \frac{\left[f^{exp}_{closed}(t_i) - f^{theo}_{closed}(t_i)\right]^2}{\sigma_i^2}\right) \qquad (7)$$

where N denotes the number of data points, f^{exp} corresponds to the experimentally determined fraction of closed particles, f^{theo} corresponds to the fraction of closed particles given by Equation 5 for each k_{close} value. The errors σ used in the calculation of the reduced χ^2–value are from repeat measurements, with an additional global error of 1%. All fitting procedures were performed with custom written Matlab (Matlab 2015, The MathWorks Inc., Natick, MA, USA) scripts using 'fminsearch' as optimization function.

Bricks. Heterodimerization kinetics of the DNA origami bricks were modelled as an irreversible bimolecular reaction:

$$A_1 + A_2 \xrightarrow{k_{on}} B$$

$$(8)$$

where A_1 and A_2 correspond to the brick monomer variants where either the protruding stacking pattern (1) or the recessed stacking pattern (2) had been activated, B denotes the dimer state and k_{on} describes the association reaction rate constant in $M^{-1}\cdot s^{-1}$. For our experimental conditions with an equimolar mixing ratio of A_1 and A_2 (with an initial concentration of A_0) and in the absence of dimers B at $t_0 = 0$, the time dependent relative concentrations of heterodimeric bricks as a function of time is given by:

$$\frac{B(t)}{A_0} = 1 - \frac{1}{1 + A_0\, k_{on}\, t} \qquad (9)$$

The model defined by Equation 9 was used to fit the fraction of dimers derived from the SAXS data for initial monomer concentrations ($A_1(t_0) = A_2(t_0) = A_0$) of 50 nM and 100 nM. We obtained an association rate constant k_{on} of 1.8 x 10^4 $M^{-1}\cdot s^{-1}$ and 1.6 x 10^4 $M^{-1}\cdot s^{-1}$ for a monomer concentration of 50 nM and 100 nM, respectively, and hence a mean value of 1.7 x 10^4 $M^{-1}\cdot s^{-1}$.

We also applied a bimolecular reaction model fit including the dissociation reaction rate constant for different final states of dimer fractions varying between 90 % and 100 % where a value of 100 % dimers resulted in the lowest χ^2-value and a negligible small value for the dissociation reaction rate constant in line with previous experiments[3]. Assuming 100 %

dimers, we tested different k_{off} rates, yielding that the fit results are insensitive towards the off-rate for $k_{off} < 10^{-6}$. Larger k_{off} values resulted in increasing χ^2-values.

To compare these values with a reaction, only limited by the diffusion dynamics of the monomeric bricks, we calculated the theoretical diffusion-limited association rate constant k_{diff} of the bricks:[10]

$$k_{diff} = 4\pi \cdot R \cdot D \cdot N_A \tag{10}$$

with R as distance within the two monomers react and form a dimer and can be assumed to be ~2 nm[11], D is the diffusion coefficient according to Equation 11 and N_A as the Avogadro constant.

SUPPORTING TEXT

Estimation of the timescales involved in the conformational transition from the open to the closed conformation of switchD16 samples.

We estimate the timescales for several processes involved in the conformational transition from the open to the closed state of the switch device. Specifically, we obtain rough, order-of-magnitude, estimates for the timescales of i) the diffusional motion of the two arms from the open to the closed conformation, ii) the formation of DNA basepair stacking interactions, and iii) the local conformational transitions of the central Holliday junction.

Diffusion of the switchD16 arms. After introducing a sufficiently high salt concentration to screen the (long-range) electrostatic repulsion that causes the switchD16 device to adopt the open conformation at low salt, we expect the transition from the open to the closed state to be fundamentally limited by diffusion of the arms, since the favourable stacking interactions that keep the switchD16 device in the closed conformation are short-range in nature[11] (with a range of $\leq$ 2.5 nm) and will only form once the arms are in sufficiently close proximity. Therefore, the timescale for diffusive motion of the two arms is expected to set the ultimate speed limit for closing of the switch device, similar to what has been observed for proteins.[12,13]

To assess the order of magnitude of the timescale for diffusive motion of the arms from the open to the closed state of switchD16, we applied a simple model based on rotational and translational diffusion. Each arm was considered as a rigid rod with a length L = 95 nm and a diameter of D = 16 nm (**Supporting Figure S4**) and the translational (D_t) and rotational (D_r) diffusion coefficients were calculated following Lehner *et al.*[14]:

$$D_t = \frac{k_B T}{3\pi\eta L}\left[\ln\left(\frac{2L}{D}\right) - \xi\right] \tag{11}$$

$$D_r = \frac{3k_B T}{\pi\eta L^3}\left[\ln\left(\frac{2L}{D}\right) - \gamma\right] \tag{12}$$

where k_B is the Boltzmann constant, T the temperature in Kelvin (300 K), η the viscosity of the solvent (1 mPa·s) and ξ and γ are correction factors for the end terms taken from Tirado *et al.*[15]. The distance d each arm has to travel depends on the opening angle Θ, which has a mean value of $\sim$ 50° (**Supporting Figure S4**).[3] Translational (t_{trans}) and rotational (t_{rot}) diffusion times for each arm are given by:
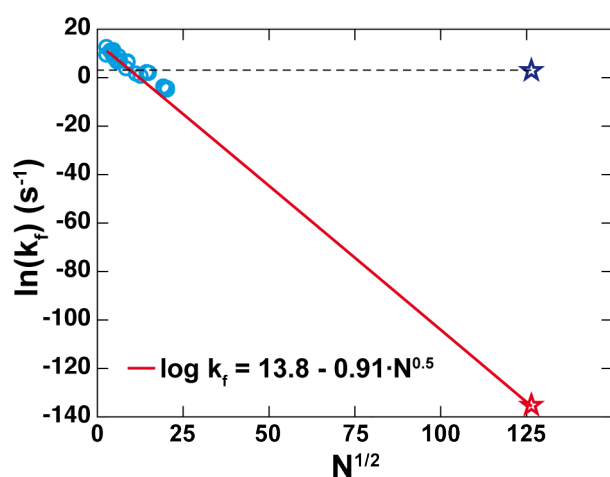
$$t_{trans} = \frac{d^2}{4\,D_t} \tag{13}$$
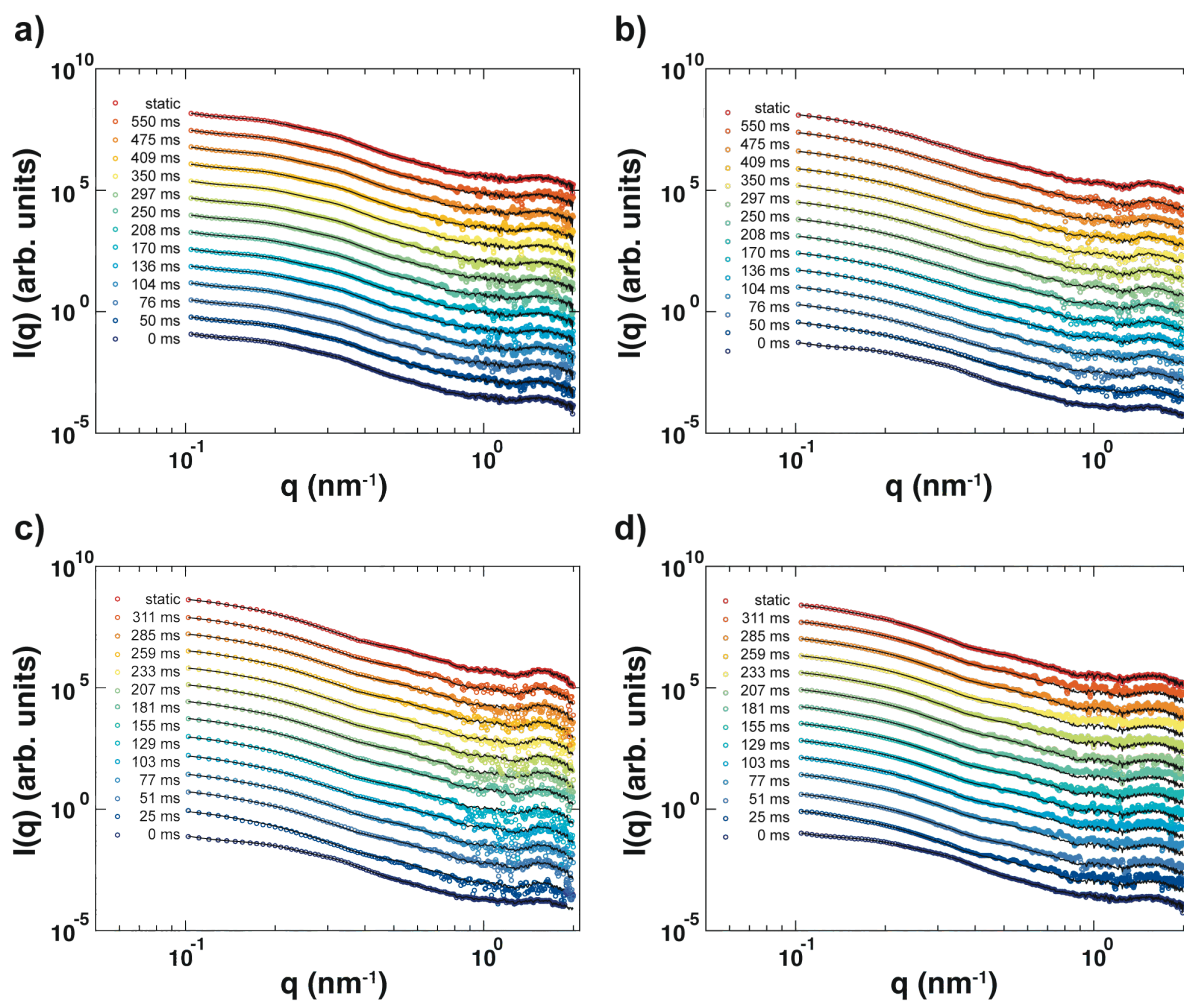
$$t_{rot} = \frac{\Theta^2}{4\,D_r} \qquad\qquad (14)$$

We find values for t_{rot} in the range of 20 to 70 µs for opening angles Θ between 50º to 90º. The estimate based on translational diffusion gives similar values, again varying the opening angle between 50º and 90º.

Formation of DNA stacking interactions. In the closed state, the two arms of the switchD16 device are held together by DNA stacking interactions. The timescale for the formation of nucleobase stacking interactions was investigated recently by force spectroscopy and molecular dynamics simulations.[11] The results suggest that formation of stacking interactions occurs on a timescale of 2.40×10^{-5} s under conditions similar to our experiments. This implies that once the arms are positioned to form stacking interactions, the formation of the short-range stacking interactions is very fast and essentially negligible compared to the timescale for diffusion of the arms or to the overall rate of closing.
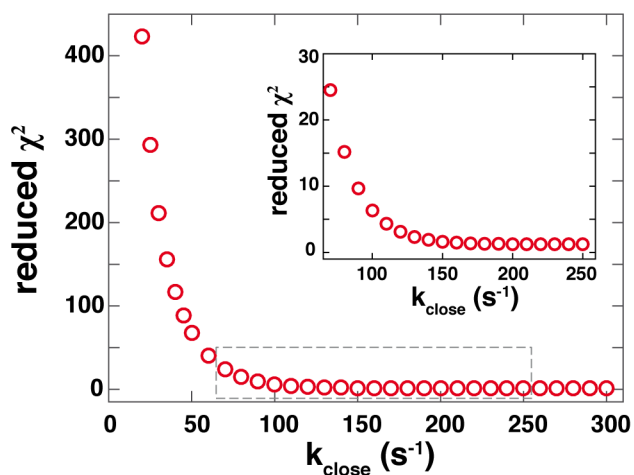
Conformational changes of the central Holliday junction. The single Holliday junction that represents the pivot point for the rotational degree of freedom of the switch object could also influence the dynamics. Dependent on the ion concentration Holliday junctions in isolation can assume multiple conformations: an open conformation at low salt conditions and two stacked conformations at high salt conditions.[16, 17] While there are several studies on the kinetics of the conformational transitions between the two possible stacked conformations of a Holliday junction,[16, 18] to the best of our knowledge there exist no experimental rate constants for the transition between the open and the stacked conformations. However, MD simulations yielded transition times in the ~µs regime, which again is much faster than the timescales for diffusional motion or overall closing and suggests that the structural dynamics of the Holliday junction are not a rate limiting factor.[19, 20]
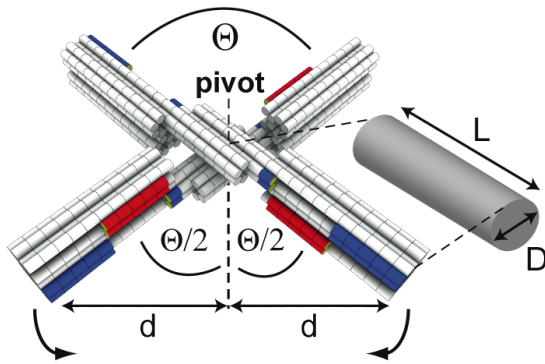
Supporting Figure S1. Scaling relationship for nucleic acid folding rate constants. Experimentally determined folding rate constants of a range of RNA molecules (cyan circles) as a function of the square root of the number of nucleotides and the corresponding fit of a scaling relationship using log k_{fold} = log (k_0) - aN^b with a, b, and k_0 as fit parameters; both the data and the fit are from Hyeon et al.[21] The red star indicates the folding rate constant predicted for the switchD16 device by the fitted scaling relationship. In contrast, the blue star corresponds to the experimentally determined folding rate constant for the transition of switchD16 from the open to the closed state at 15 mM $MgCl_2$.
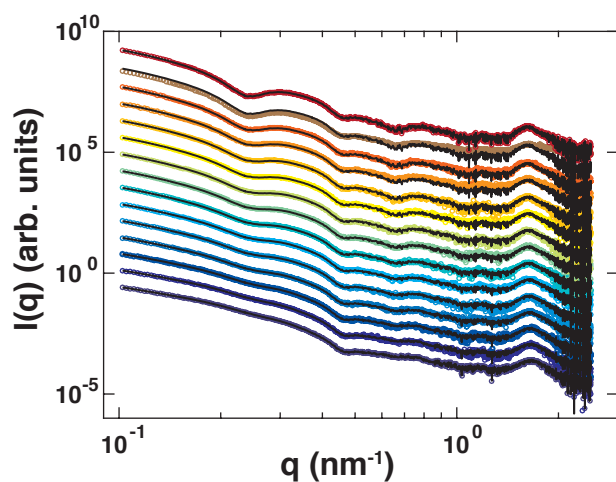
Supporting Figure S2. Time-dependent scattering profiles for switchD16 and two-state fits. Time-dependent scattering profiles of switchD16 samples upon mixing with varying $MgCl_2$ concentrations and corresponding fitted profiles from a two-state model (black lines) (see main text). **a)** Evolution of scattered intensity upon equimolar mixing of switchD16 samples with 5 mM $MgCl_2$ at different time points indicated in the legend. SAXS curves at the bottom (dark blue circles) and at the top (red circles) correspond to static reference profiles of switchD16 samples at the initial and final $MgCl_2$ concentrations (here: 5 mM). **b)** Scattering profiles for switchD16 samples diluted into a final concentration of 15 mM $MgCl_2$ at subsequent timepoints acquired after mixing. SAXS profiles at the bottom (dark blue circles) and at the top (red circles) are obtained from static SAXS measurements of switchD16 samples diluted in 5 mM and 15 mM $MgCl_2$, respectively. **c)** Scattering profiles of switchD16 samples diluted into a final concentration of 25 mM $MgCl_2$ buffer. SAXS profiles at the bottom (dark blue circles) and at the top (red circles) are obtained from static SAXS measurements of switchD16 samples diluted in 5 mM and 25 mM $MgCl_2$, respectively. **d)** Time-dependent SAXS data obtained from switchD16 samples after equimolar mixing with $MgCl_2$ buffer resulting in a final concentration of 35 mM $MgCl_2$. SAXS curves at the bottom (dark blue circles) and at the top (red circles) are obtained from static SAXS measurements of switchD16 samples diluted in 5 mM and 35 mM $MgCl_2$, respectively. Data are vertically offset for clarity. Data from trSAXS experiments with final $MgCl_2$ concentrations of 5 and 35 mM after mixing contain twice the number of data points as compared to the 15 and 25 mM $MgCl_2$ data due to interpolation to the q-bin size of static reference profiles, which where recorded with half of the bin size as stopped-flow SAXS experiments.
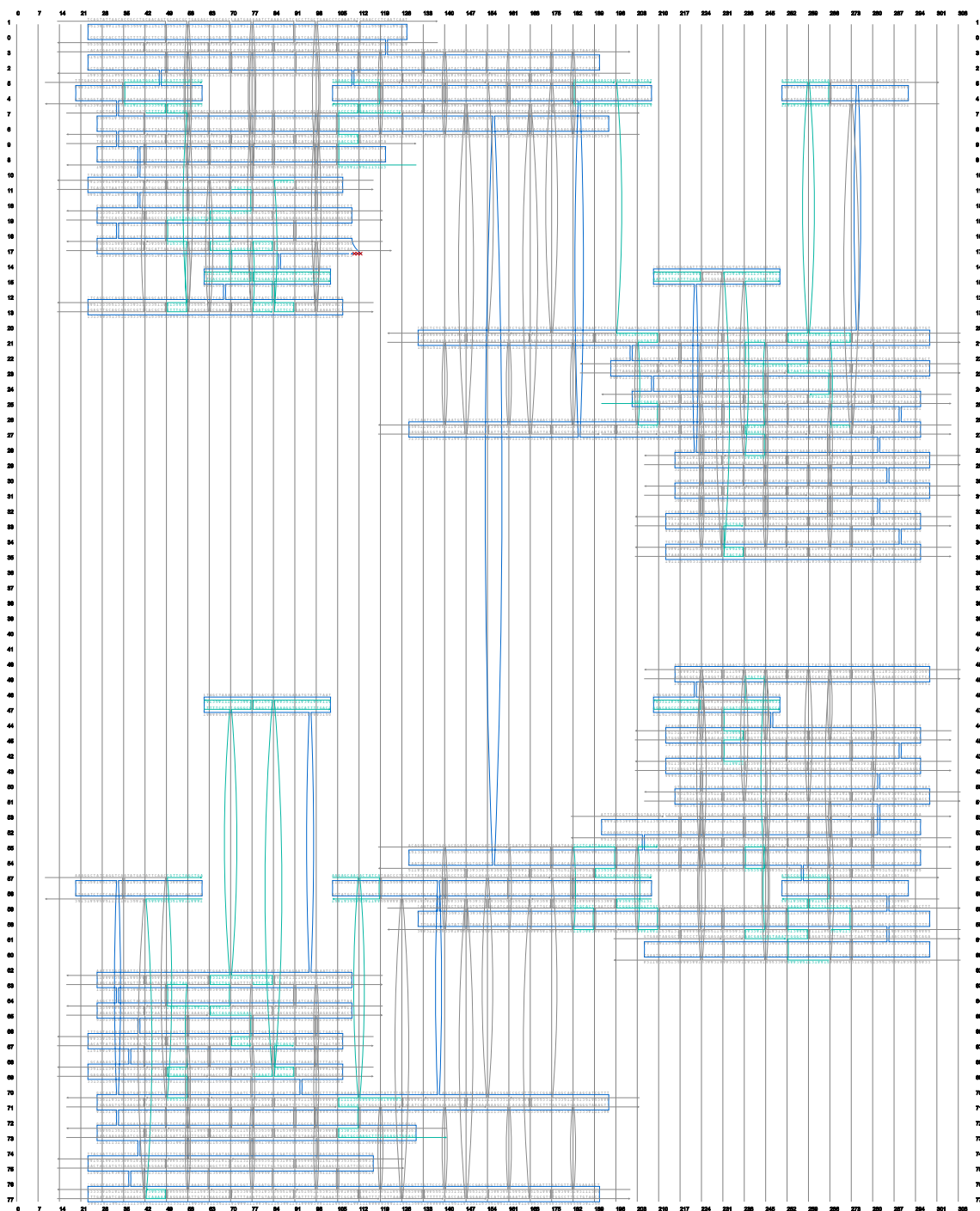
Supporting Figure S3. Estimate of the closing reaction rate constant of SwitchD16 particles for a final MgCl$_2$ concentration of 25 mM after mixing. We used Equation 5 and calculated the reduced χ^2–value for different closing rate constants while setting the opening rate constant to zero (as at a MgCl$_2$ concentration of 25 mM the closed fraction in equilibrium is ~98 %, suggesting that the opening rate constant is essentially negligible). The data are well described for k_{close} values equal or greater ~ 150 s^{-1} (see inset graph corresponding to the data range indicated by the grey frame). We found an very similar results for the 35 mM MgCl$_2$ data.
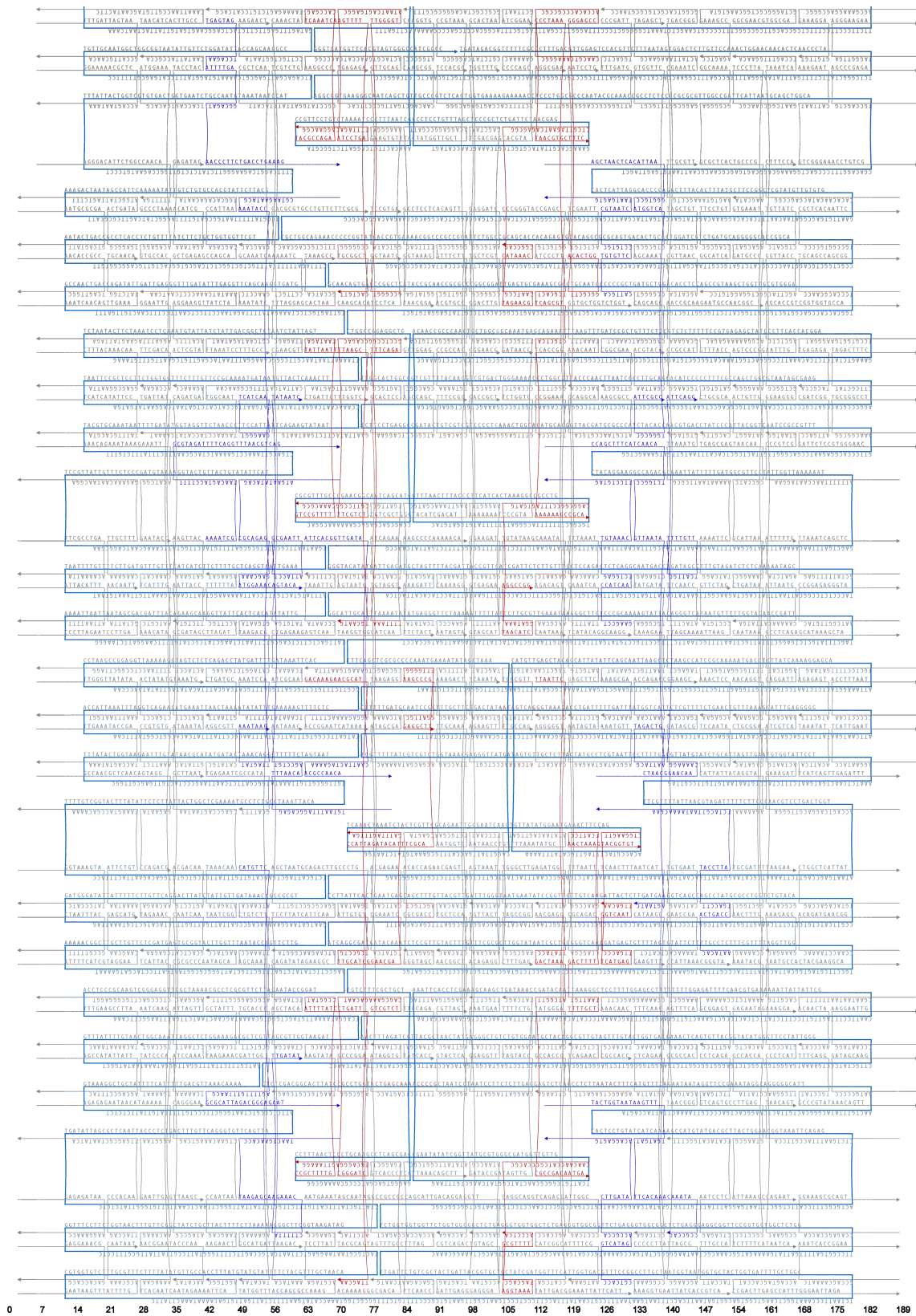
Supporting Figure S4. Schematic model and length scales used to estimate the diffusion times of the arms of switchD16 required to change from the open conformation (shown here) to the closed conformation.

Supporting Figure S5. Time evolution of scattering profiles from DNA origami dimerization kinetics after 1:1 mixing of monomeric brick samples at an initial concentration of 100 nM: 0 min (dark blue circles, bottom), 2 min, 5 min, 10 min, 15 min, 20 min, 30 min 45 min, 60 min, 90 min, 2 h, 3 h, 4 h 30 min, 12h 30 min and 24 h (red circles, top). Black lines correspond to fits from a two-state model following Equation 1.

Supporting Figure S6. Strand diagram of the dynamic (switchD16) variant. Scaffold (shown in blue) and staple layout of the dynamic switch variant with 16 activated stacking interactions. Cyan: stacking activated. Generated with caDNAno v0.2.

Supporting Figure S7. Stand diagram of brick monomer A$_1$ generated with caDNAno v0.2.

Supporting Figure S8. Strand diagram of brick monomer A₂ generated with caDNAno v0.2.

SUPPORTING REFERENCES

(1)   Kick, B.; Praetorius, F.; Dietz, H.; Weuster-Botz, D. *Nano Lett.* **2015,** 15, 4672-6.

(2)   Douglas, S. M.; Marblestone, A. H.; Teerapittayanon, S.; Vazquez, A.; Church, G. M.; Shih, W. M. *Nucleic Acids Res.* **2009,** 37, 5001-6.

(3)   Gerling, T.; Wagenbauer, K. F.; Neuner, A. M.; Dietz, H. *Science* **2015,** 347, 1446-52.

(4)   Bruetzel, L. K.; Gerling, T.; Sedlak, S. M.; Walker, P. U.; Zheng, W.; Dietz, H.; Lipfert, J. *Nano Lett.* **2016,** 16, 4871-9.

(5)   Sobczak, J. P.; Martin, T. G.; Gerling, T.; Dietz, H. *Science* **2012,** 338, 1458-61.

(6)   Stahl, E.; Martin, T. G.; Praetorius, F.; Dietz, H. *Angew. Chem., Int. Ed. Engl.* **2014,** 53, 12735-40.

(7)   Blanchet, C. E.; Spilotros, A.; Schwemmer, F.; Graewert, M. A.; Kikhney, A.; Jeffries, C. M.; Franke, D.; Mark, D.; Zengerle, R.; Cipriani, F.; Fiedler, S.; Roessle, M.; Svergun, D. I. *J. Appl. Crystallogr.* **2015,** 48, 431-443.

(8)   Panine, P.; Finet, S.; Weiss, T. M.; Narayanan, T. *Adv. Colloid Interface Sci.* **2006,** 127, 9-18.

(9)   Guinier, A., *La diffraction des rayons X aux trés petits angles: application a l'étude de phénomènes ultramicroscopiques.* Annales de Physique: Paris, 1939.

(10)   Atkins, P. W.; de Paula, J., *Atkins' Physical Chemistry.* Oxford University Press: USA, 2002.

(11)   Kilchherr, F.; Wachauf, C.; Pelz, B.; Rief, M.; Zacharias, M.; Dietz, H. *Science* **2016,** 353.

(12)   Yang, W. Y.; Gruebele, M. *Nature* **2003,** 423, 193-7.

(13)   Kubelka, J.; Hofrichter, J.; Eaton, W. A. *Curr. Opin. Struct. Biol.* **2004,** 14, 76-88.

(14)   Lehner, D.; Lindner, H.; Glatter, O. *Langmuir* **2000,** 16, 1689-1695.

(15)   Tirado, M. M.; Martínez, C. L.; la Torre, J. G. d. *J. Chem. Phys.* **1984,** 81, 2047-2052.

(16)   McKinney, S. A.; Declais, A. C.; Lilley, D. M.; Ha, T. *Nat. Struct. Biol.* **2003,** 10, 93-7.

(17)   Joo, C.; McKinney, S. A.; Lilley, D. M.; Ha, T. *J. Mol. Biol.* **2004,** 341, 739-51.

(18)   Overmars, F. J.; Altona, C. *J. Mol. Biol.* **1997,** 273, 519-24.

(19)   Yu, J.; Ha, T.; Schulten, K. *Nucleic Acids Res.* **2004,** 32, 6683-95.

(20)   Wang, W.; Nocka, L. M.; Wiemann, B. Z.; Hinckley, D. M.; Mukerji, I.; Starr, F. W. *Sci. Rep.* **2016,** 6, 22863.

(21)   Hyeon, C.; Thirumalai, D. *Biophys. J.* **2012,** 102, L11-3.